Hindawi
Advances in Materials Science and Engineering
Volume 2022, Article ID 9444524, 11 pages
https://doi.org/10.1155/2022/9444524

Research Article

Influence of Silicon Dioxide-Titanium Dioxide Antireflective Electrosprayed Coatings on Multicrystalline Silicon Cells

Rajasekar Rathanasamy,[1] Gobinath Velu Kaliyannan,[2] Santhosh Sivaraj,[3] Abishek Saminathan,[1] Bharathikannan Krishnan,[1] Dhayananth Palanichamy,[1] and Md. Elias Uddin [4]

[1]*Department of Mechanical Engineering, Kongu Engineering College, Perundurai, Tamil Nadu 638060, India*
[2]*Department of Mechatronics Engineering, Kongu Engineering College, Perundurai, Tamil Nadu 638060, India*
[3]*Department of Robotics and Automation, Easwari Engineering College, Ramapuram, Chennai, Tamil Nadu 600089, India*
[4]*Department of Leather Engineering, Faculty of Mechanical Engineering, Khulna University of Engineering and Technology, Khulna, Bangladesh*

Correspondence should be addressed to Md. Elias Uddin; eliasuddin@le.kuet.ac.bd

Received 30 May 2022; Revised 30 July 2022; Accepted 29 August 2022; Published 8 October 2022

Academic Editor: Guang Xing Liang

This research work primarily focuses on enhancing the power conversion efficiency (PCE) of polycrystalline silicon solar cells by using a single-layer and a double-layered antireflection coating deposited through the electrospraying technique. The usage of titanium dioxide and silicon dioxide as antireflection coating materials has shown a significant increase in the optical and electrical properties of solar cells under open and controlled light sources. The sample with TiO_2 as a base layer and SiO_2 as the top layer (sample B-IV) exhibited a maximum PCE of 18.90% in direct sunlight and 21.19% in a neodymium setup with cell temperatures of 40°C and 52.1°C, respectively. Sample B-IV has also shown the lowest resistivity of $3.1 \times 10^{-3}\ \Omega\cdot$cm among the coated samples. Also, an increase of 11.6% light transmittance and a reduction of 9.6% light reflectance were exerted by sample B-IV. The results obtained from different analysis proves that TiO_2/SiO_2 was an appropriate antireflection coating material for enhancing the PCE of the polycrystalline silicon solar cell.

1. Introduction

Renewable energy is harnessed from natural sources or processes which continually replenish at a faster rate than consumption. This makes renewable energy a more efficient solution to the world's power problem [1]. The need for cleaner energy in the past decade has paved way for a promising feature in the field of solar power generation [2]. Power generation through solar energy is widely encouraged as it is cheap [3], clean [4] and nonpolluting. A polycrystalline solar cell is a type of solar cell made from various crystals of silicon fused into a single photovoltaic cell. This type of solar cell is widely used in the field of commercial power generation through solar energy. The practical efficiency of these solar cells is usually around 12–15%. The factors like humidity, dust, and reflection of sunlight play an important role in altering the efficiency of solar cells. In general, 20–30% of sunlight gets reflected from the surface of the solar cell [5]. The reflection losses in the polycrystalline solar cells can be reduced by increasing the power conversion efficiency (PCE) with the help of an antireflection coating [6]. For antireflection coating, a variety of materials can be employed like ZnO [7], SiO_2 [8], TiO_2 [9], Al_2O_3 [10], and ZnS [11]. In this research work, SiO_2 and TiO_2 have been chosen as antireflection coating (ARC) materials for minimising the incident light reflection and thereby increasing the power conversion efficiency of solar cells. SiO_2 was chemically stable at high temperatures and has scratch resistance properties [12]. TiO_2 exhibits mechanical hardness, chemical stability, and less moisture absorption and has a suitable refractive index and minimum absorption throughout the visible spectra region of solar cells. The refractive indices of SiO_2 and TiO_2 were 1.44 and 2.20, respectively [13]. Four different coated samples were prepared, B-II (SiO_2), B-III (TiO_2), B-IV (TiO_2/SiO_2), B-V (SiO_2/TiO_2), and B-I as uncoated solar cells [14]. The antireflection coating had been deposited by various methods such as spin coating [15], slot die coating [16], electrospraying [17], doctor blading [18], dip coating [19], and sputter deposition [5]. The electrospraying method is preferred for this research work as it has already been extensively employed in various applications including film coating, drug delivery [20], chocolate processing [21], and encapsulation of nutraceuticals [22]. In electrospraying, both size and generation of the droplet can be controlled through the supplied voltage at the capillary nozzle and the flow rate of the liquid which enables the desired output of deposition of the ARC material.

This research work aims in utilising TiO_2 and SiO_2 as the ARC material to increase the PCE of polycrystalline silicon solar cells by electrospraying technique. The necessary analysis was carried out to determine the effects of TiO_2 and SiO_2 coating on the optical, structural, electrical, and thermal properties of the coated samples. The coated polycrystalline Si solar cells were inspected under sunlight source and neodymium light sources.

2. Materials Used

Precursors—titanium dioxide (TiO_2) and silicon dioxide (SiO_2) with 99.9% purity were procured from Sigma–Aldrich. Ethanol (C_2H_5OH) with 99.9% purity was bought from Changshu Hongsheng Fine Chemicals, China. Polycrystalline silicon solar cells were bought from Eco Worthy, China.

2.1. Methodology. The components involved in electrospraying are a liquid feeder (syringe), a blunt hypodermic needle, and a high voltage source [23]. The overall coating processes were represented in Figure 1. The voltage applied to the droplets for electrospraying is typically between 5 kV and 30 kV of positive polarity. The antireflection coating material was completely dissolved in ethanol using a magnetic stirrer. The target solar cell was mounted over a flat plate covered with aluminium foil. The mass flow rate and supplied voltage were configured in the electrospraying machine as 2 ml/h and 17 kV, respectively. The overall operating parameters for achieving electrosprayed antireflective thin surface films were indicated in Table 1. The ARC solution in the syringe was charged and dispersed as fine droplets towards the target solar cell. The droplets formed a coating on the surface of the solar cell as a result of the strong electrostatic force. As indicated in Table 1, the coated samples were specified as B-II, B-III, B-IV, and B-V representing the single layer TiO_2, single layer SiO_2 coating, double layer of TiO_2/SiO_2, and double layer of SiO_2/TiO_2 samples, respectively, whereas, B-I indicates the uncoated polycrystalline silicon solar cell.

2.2. Characterisation Techniques. FESEM (Field Emission Scanning Electron Microscopy) analysis was a strong investigative tool used to study the surface morphology and cross-sectional of the coated and uncoated samples [24], Chemical composition of the coated solar cells was examined through the energy dispersive X-ray analysis (EDAX). The film thickness and surface topography of the coated and uncoated polycrystalline samples were recorded using AFM (Atomic Force Microscopy) analysis. The current-voltage characteristics of the solar cells were measured by using I–V analysis with the help of Keithley 2450 source metres in both controlled and uncontrolled source environments. The influence of the coating over the solar cells and the optical properties of the cells were observed through the optical transmittance and reflectance analysis.

3. Result and Discussion

The surface morphology and cross-section thickness of the coated thin films were analysed using FESEM. The coating structure and the coating thickness of sample B-IV are displayed in Figure 2. The cross-sectional thickness of the coated layers in samples B-II, B-III, B-IV, and B-V were observed to be 247 nm, 360 nm, 610 nm, and 762 nm, respectively. Various parameters impact the quality of the coating such as flow rate, supplied voltage, and distance between the substrate and nozzle. The optical coating thickness was determined to be 610 nm for sample B-IV with titanium dioxide as a base layer and silicon dioxide as the top layer. The sample B-IV has performed exceptionally by exhibiting maximum PCE in the I–V analysis.

Through EDAX, the chemical composition of the coated material on the surface of the solar cell was determined. The EDAX graph of sample B-IV is displayed in Figure 3, which confirms the presence of both silicon and titanium elements on the surface of solar cells. Surface roughness plays a significant role in trapping solar light as rough surfaces lead to more light trapping capacity. The surface topography of the coatings was analysed through AFM analysis. The AFM result (Figure 4) was used to determine the surface roughness values of coated samples B-II, B-III, B-IV, and B-V to be 93 nm, 108 nm, 121 nm, and 129 nm, respectively.

Under the influence of antireflective surface coatings, more incident light gets trapped by minimising the light reflectance. The incident light rays were found to be constructive or destructive which was purely dependent on the thickness of the antireflective layer [25]. Until reaching the optimal coating thickness, the incident light gets coupled together and then reaches the depletion region. Beyond the optimal coating thickness, the incoming light was found to exert destructive interference [26]. Hence, a lesser number of photons reaches the depletion region resulting in a decrement in the power generation ability of solar cells. For obtaining the effective antireflective property, amplitudes of reflected beam at a coated thin film—air interface and coated thin film—substrate interface should be equal and 180° out of phase [27]. This results in destructive interference of reflected beams. There are two important conditions with

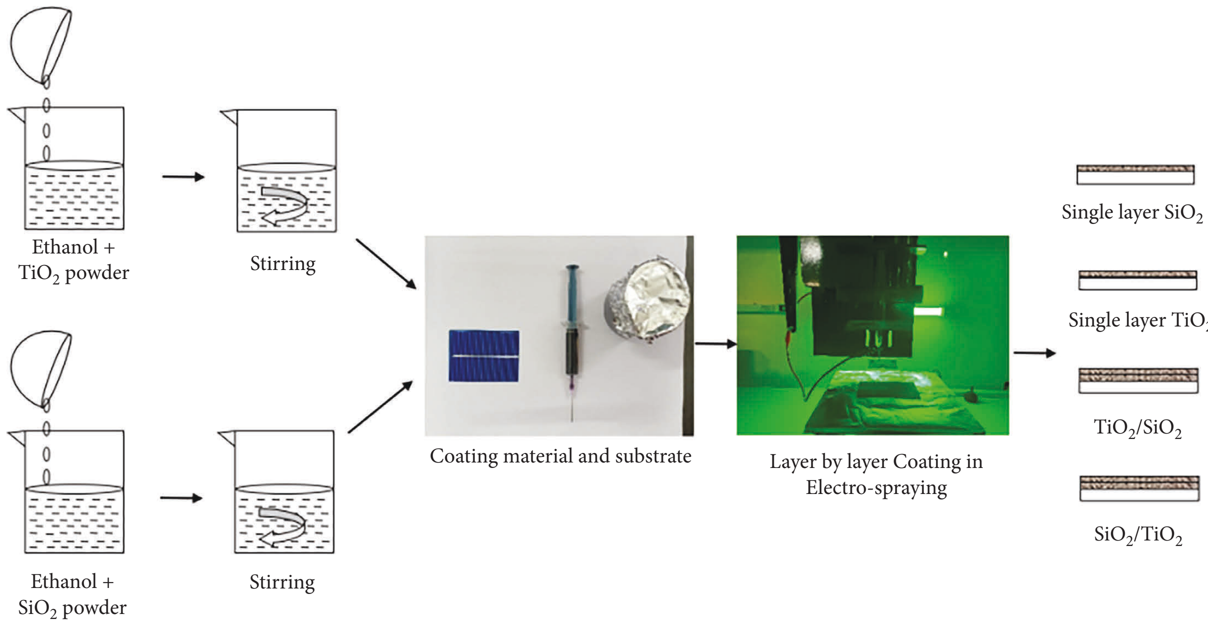

Figure 1: Pictorial representation of electrospraying method.

Table 1: Sample description and maintained coating parameters.

Sample	Coating material	Flow rate (ml/h)	Voltage (kV)	Substrate target distance (cm)
B-II	SiO_2	2	17	3
B-III	TiO_2			
B-IV	TiO_2/SiO_2			
B-V	SiO_2/TiO_2			

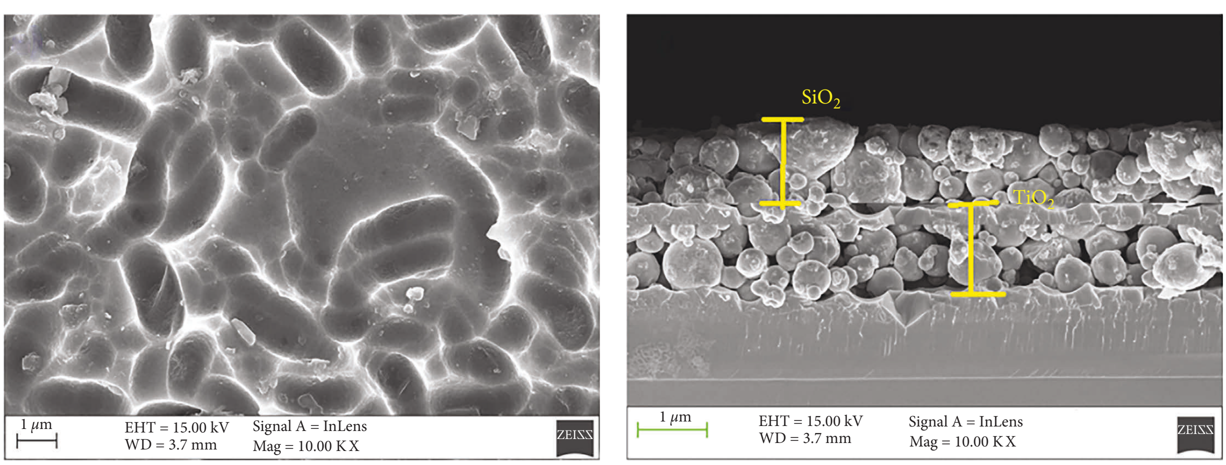

(a) (b)

Figure 2: (a) Surface morphology of B-IV (TiO_2/SiO_2). (b) Cross-section of B-IV (TiO_2/SiO_2) solar cells.

which the optimal thickness of the antireflective coating can be evaluated (as indicated in equations (1) and (2)).

(i) The product of refractive indices of the coated substrate (n_0) and working medium (n_2) must be equal to the square of the refractive index of the deposited antireflective film (n_1).

$$n_1 \sqrt{n_0 \times n_2}. \quad (1)$$

(ii) The optimal thickness of antireflective film must be equal to one-fourth of the wavelength at which minimal reflectance is obtained.

$$n \times t = \frac{\lambda_{min}}{4}. \quad (2)$$

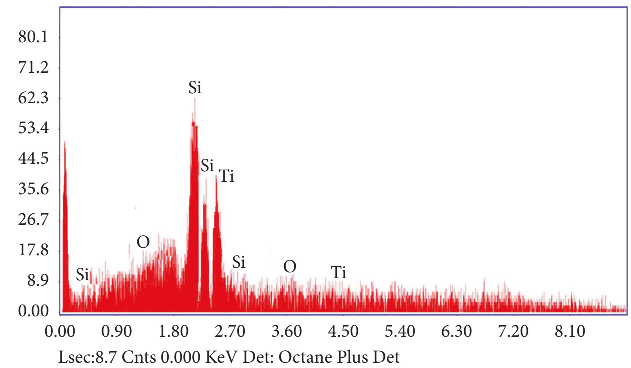

Figure 3: Energy dispersive X-ray analysis (EDAX) of B-IV sample coated solar cell.

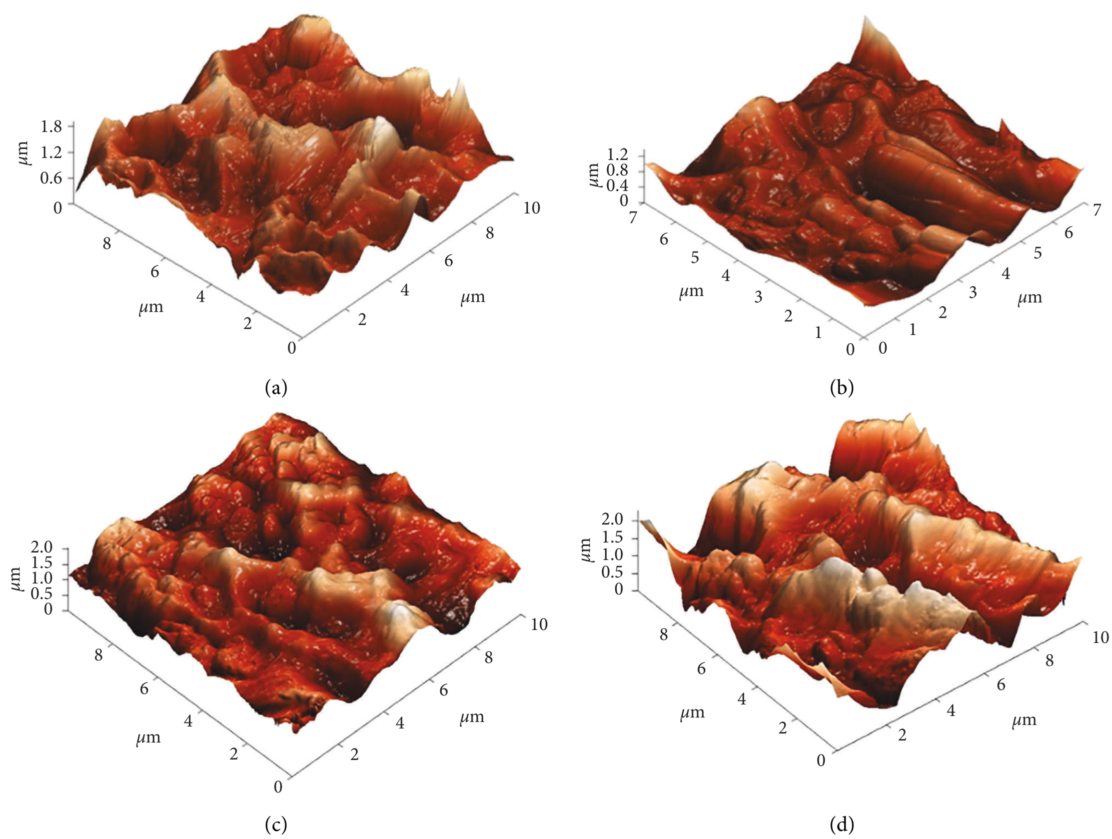

Figure 4: 3D AFM image of coated solar cell samples (a) B-II, (b) B-III, (c) B-IV, (d) B-V.

The thickness at which zero reflectance was achieved at ≈ 610 nm for the B-IV sample with a refractive index of 2.16. Constructive interference of reflected beams tends to arise beyond the optimal coating thickness of the antireflective surface.

The sample B-IV (TiO_2/SiO_2) exhibited higher transmittance of 95.5% in the UV visible region compared to other samples in the visible UV spectrum. This was due to the minimised reflective losses in the sample. The rough surface and optimal thickness of the coating reduced the scattering of light from the surface and resulted in higher transmittance. The presence of Ti and Si enabled more photons from the incident light to pass through the coated samples. This phenomenon was evident from obtained optical studies of coated samples (as shown in Figures 5 and 6), whereas, the sample B-V (SiO_2 as a base layer) revealed comparatively low transmittance than B-IV (TiO_2 as a base layer which can be correlated with the excessive thickness of the coated layer. The consolidated transmittance and reflectance values observed in the optical analysis are tabulated in Table 2.

I–V analysis for the coated solar cells and the bare solar cell was conducted in both controlled and uncontrolled open environments to learn the influence of the coating on the electrical properties of the solar cells. In an open-source environment, the analysis was done under direct sunlight using a Keithley source metre, power source metre, and kickstart interfacing software. The power output generated

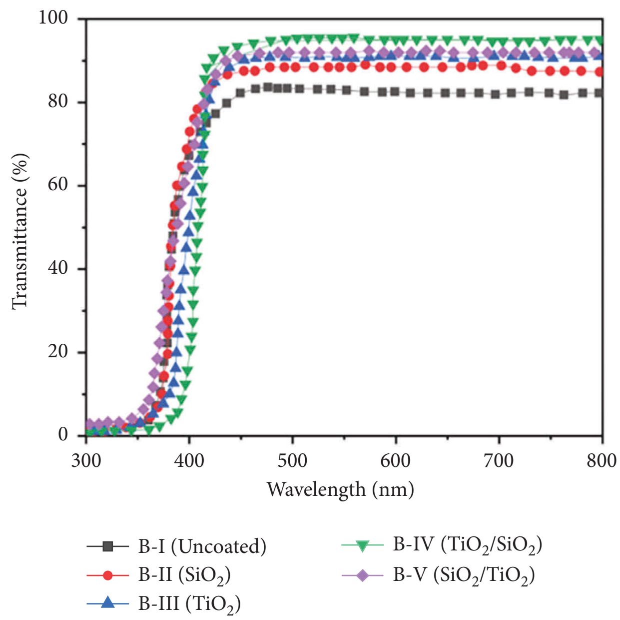

FIGURE 5: Optical transmittance spectra of various solar samples.

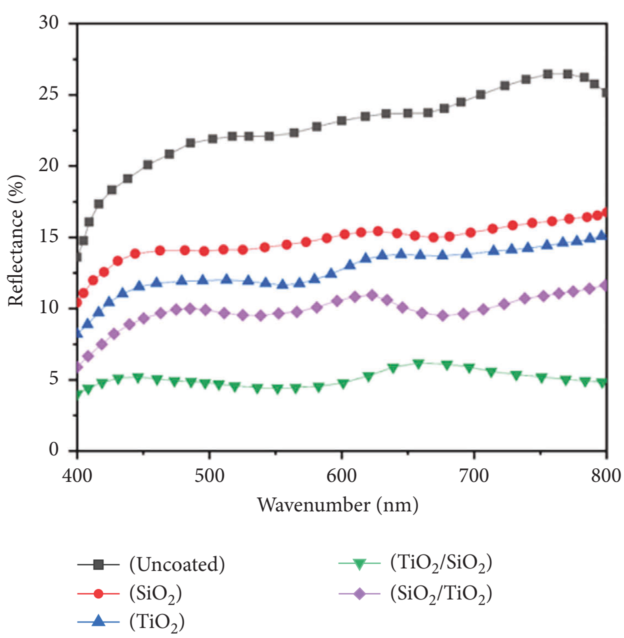

FIGURE 6: Optical reflectance spectra of various solar samples.

by the samples' direct sunlight is tabulated in Table 3. The results of the I–V analysis imply that the efficiency of the solar cells increases with the increase in short circuit photocurrent density and open circuit voltage. Sample B-IV has shown maximum current density and open circuit voltage of 36.46 mA/cm^2 and 0.656 V leading to a maximum efficiency of 18.90% (Figure 7).

A neodymium lamp was used as a source of illumination in the controlled source environment which can emit radiation similar to the sunlight. Measured I–V values of the coated samples under closed source were tabulated in Table 4. The sample B-IV experiences superior results in a closed environment with 21.19% PCE (Figure 8). As expected, a decline in the power output of sample B-V was observed. The sample B-V is confirmed to have exceeded coating thickness and roughness values than the optimal level. The solar cell samples performed better in the fabricated neodymium setup than in direct sunlight. The source of illumination in the controlled setup emits constant radiation for the solar cell without any fluctuation. However, in direct sunlight, the radiation is subjected to variation with time due to several factors.

The simulation results for various coated and uncoated solar cells under consistent light incidence. The simulation was carried out for antireflective coated multicrystalline silicon solar cells using SCAPS software. The best operating solar cells that exert maximum cell performance were represented in Figure 9. However, the experimental results were found to be lesser compared to simulation results, due to certain errors such as calibration errors, uncontrolled temperature change, deposition of light inhibitor layers (dust particles), minor internal cracks, and resistive losses [28]. Among all other coated solar cells, B-IV solar cells exert maximum photocurrent generation. For B-IV solar cells, the simulation results were obtained as maximum Voc, Isc, and PCE as0.664 V, 41.85 mA/cm^{2,} and 22.06% (simulated under constant light illumination). Increment in electron-hole pair generation leads to an increase in the power conversion efficiency of photovoltaic cells. As a counteraction, electron-hole pair recombination does not improve power conversion efficiency. Instead, the photon gets expelled while the electron falls from conduction to the valence band. Such a recombination process was known as the radiative-recombination process [29].

The resistivity of the coated samples was inspected through the four-probe technique. Double coated solar cells had considerably low resistivity and sample B-IV held the lowest resistivity of $3.1 \times 10^{-3}\ \Omega$·cm. The SiO_2coated sample experienced the highest resistivity among the coated solar cells, but it was still lower than the resistivity of the uncoated solar cell. This reduction in the resistivity was due to the increase in the carrier concentration and Hall mobility which was illustrated in Figure 9. The conductivity and photo-generated current get increased for the multilayer antireflective coated solar cell (B-IV) than in other solar cells. With the decrement in measured resistivity of coated solar cells, Hall mobility and carrier concentration gets increased as compared to the bare solar cell. The mobility of electrons was improved by the larger-sized grains with lesser grain boundary leads to enhanced photocurrent generation [30]. The Hall mobility and carrier concentration were determined using the following equations (3) and (4) The measured electrical characteristics of various solar cells were represented in Figure 10.

$$n_H = \frac{1}{e \times R_H}, \tag{3}$$

$$\mu_H = R_H \times \sigma, \tag{4}$$

where n_H = Carrier concentration (cm^{-3}), μ_H = Hall mobility (cm^2/VS), e = Charge of an electron, R_H = Hall coefficicent

Table 2: Transmittance and reflectance of coated and uncoated solar cells.

Sample	Coating material	Coating thickness (nm)	Transmittance (%)	Reflectance (%)
B-I	Uncoated	0	83.9	13.6
B-II	SiO_2	247	87.6	10.4
B-III	TiO_2	360	90.3	8.2
B-IV	TiO_2/SiO_2	610	95.5	4
B-V	SiO_2/TiO_2	762	93.1	5.9

Table 3: Measured values of samples under direct sunlight.

Samples	Open circuit voltage (V)	Short circuit current density (mA/cm^2)	Fill factor (%)	Power conversion efficiency (%)
B-I (uncoated)	0.628	31.03	0.746	14.54
B-II (SiO_2)	0.631	33.4	0.75	15.81
B-III(TiO_2)	0.635	34.7	0.78	17.19
B-IV (TiO_2/SiO_2)	0.656	36.46	0.79	18.90
B-V (SiO_2/TiO_2)	0.649	35.5	0.77	17.74

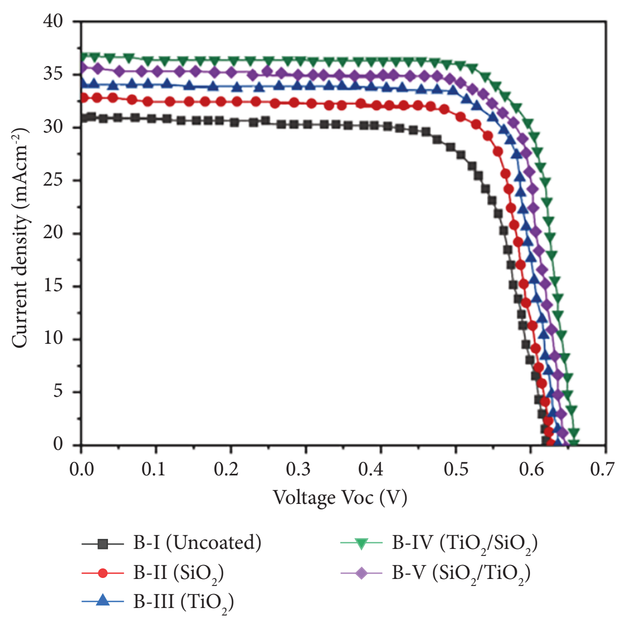

Figure 7: Measured values of the samples under direct sunlight.

Table 4: Measured values of samples under a controlled source of environment.

Samples	Open circuit voltage (V)	Short circuit current density (mA/cm^2)	Fill factor (%)	Power conversion efficiency (%)
B-I (uncoated)	0.632	32.16	0.73	14.84
B-II (SiO_2)	0.634	36.1	0.75	17.17
B-III (TiO_2)	0.64	38.97	0.76	18.96
B-IV (TiO_2/SiO_2)	0.658	40.76	0.79	21.19
B-V (SiO_2/TiO_2)	0.652	40.02	0.77	20.09

(cm^3/coulomb), σ = electrical conductivity of coated thin films.

The bare cell and coated samples were analysed in accordance with the heat flux measurement using a Fluke—thermal imager in both controlled and uncontrolled environments as indicated in Figures 11 and 12. The thermal analysis revealed that the efficiency of solar cells depends on the temperature of the solar cell. Also, the increase in heat flux increases the resistivity in solar cells and affects the power generation of the solar cell [31, 32]. Sample B-IV exhibited lower temperatures of 40.0°C and 39.6°C compared to other samples in both controlled and

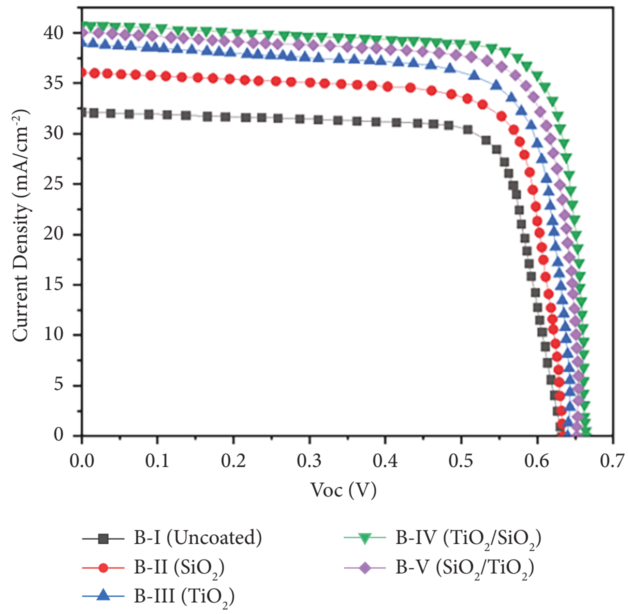

Figure 8: Measured values of the samples under a controlled environment.

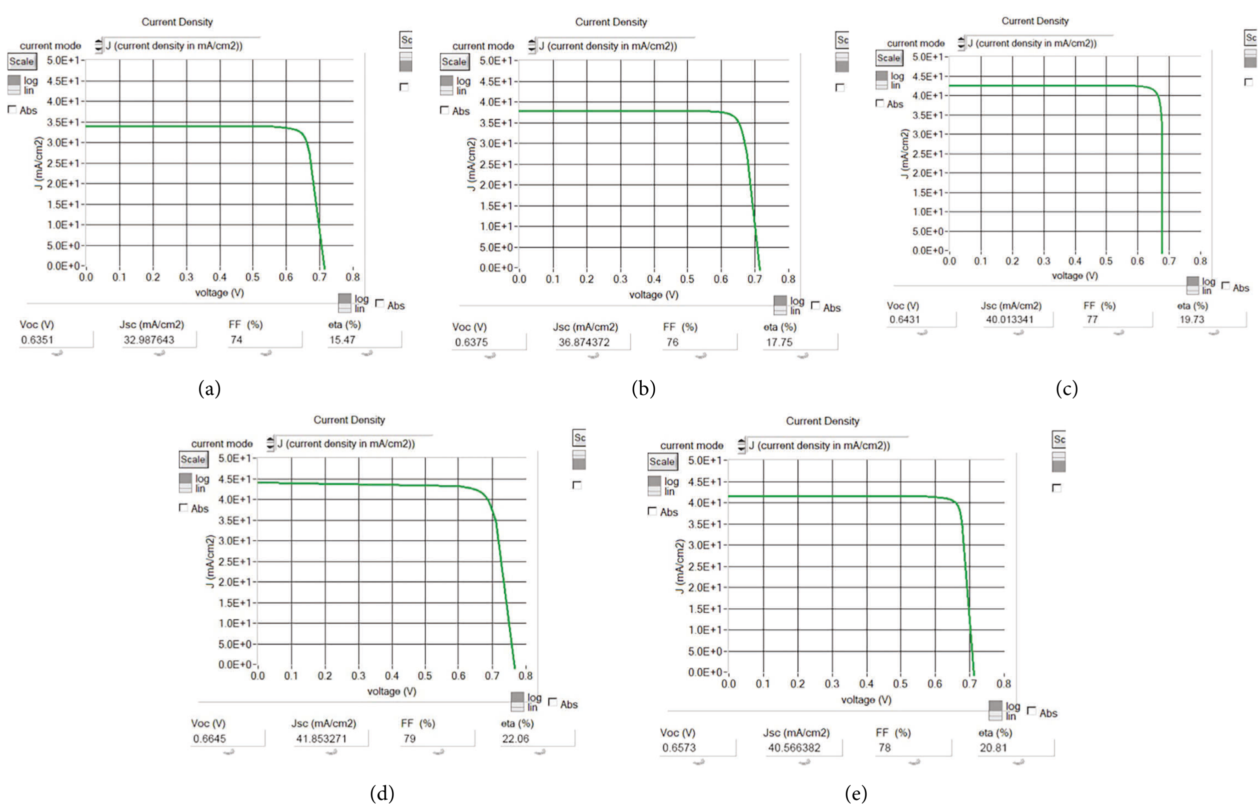

Figure 9: Simulation results of various coated and uncoated solar cells: (a) B-I; (b) B-II; (c) B-III; (d) B-IV; (e) B-V.

uncontrolled source environments, respectively. The temperature of samples decreases from B-I to B-IV, whereas sample B-V possessed an elevated temperature than expected. The sample with SiO_2 as a base layer could not provide better thermal properties than the sample with TiO_2 as a base layer. From the analysis of thermal, electrical, and structural properties of the coated solar cells, the double-layered coating of TiO_2/SiO_2 acts as excellent antireflective coating elements for increasing the PCE of polycrystalline silicon solar cells.

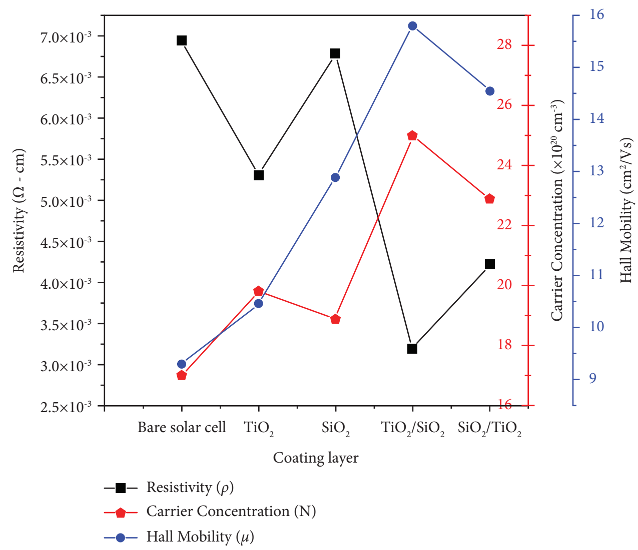

FIGURE 10: Electrical characteristics of uncoated and coated samples.

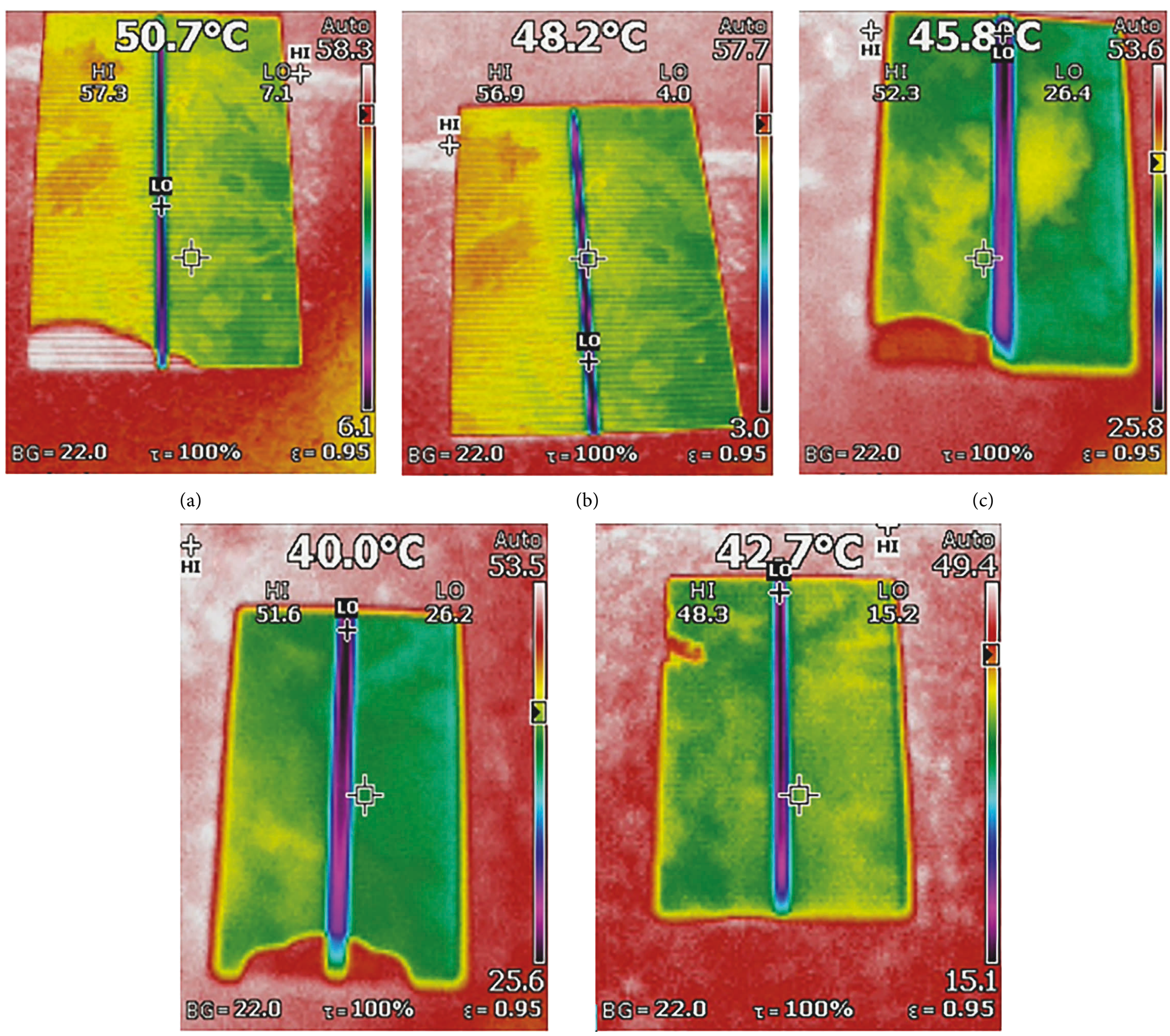

(a) (b) (c) (d) (e)

FIGURE 11: Thermal analysis under controlled source environment: (a) B-I (uncoated), (b) B-II (SiO_2), (c) B-III (TiO_2), (d) B-IV (TiO_2/SiO_2), and (e) B-V (SiO_2/TiO_2).

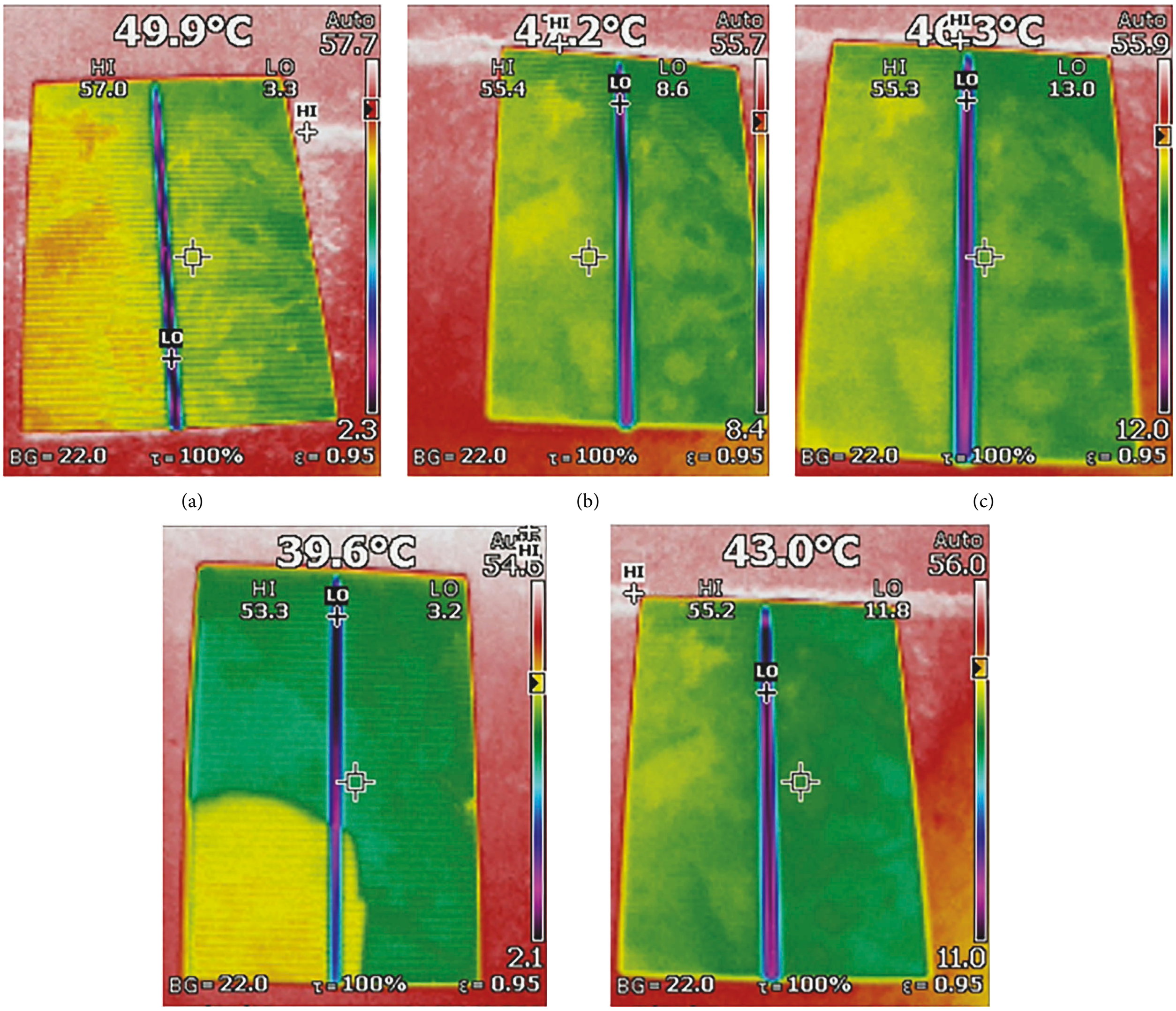

(a) (b) (c)

(d) (e)

Figure 12: Thermal analysis under direct sunlight: (a) B-I (uncoated), (b) B-II (SiO_2), (c) B-III (TiO_2), (d) B-IV (TiO_2/SiO_2), and (e) B-V (SiO_2/TiO_2).

4. Conclusion

Antireflection coating materials were prepared using titanium dioxide and silicon dioxide and employed on the solar cells through the electrospraying method. The samples were prepared with two single-layered coatings and two double-layered coatings. The cross-sectional thickness of the coated layer in samples B-II, B-III, B-IV, and B-V was observed to be 247 nm, 360 nm, 610 nm, and 762 nm, respectively. The results from EDAX confirm the proper deposition of TiO_2& SiO_2 elements on the samples. The surface roughness values of the samples B-II, B-III, B-IV, and B-V were reckoned to be 93 nm, 108 nm, 121 nm, and 129 nm. Sample B-IV has shown a significant increase in the PCE of the solar cell with 18.90% of efficiency under direct sunlight and 21.19% in a controlled source environment with the highest transmittance of 95.5% and reflectance as low as 4%. The resistivity was remarkably reduced in the double-layered coated samples especially the B-IV sample had $3.1 \times 10^{-3}\,\Omega$ - cm resistivity. The temperature of the coated solar cells and the heat flux variations were observed from temperature analysis, which confirms the lowest surface temperature in both controlled and uncontrolled setup by the sample B-IV (40.0°C and 39.6°C). Hence, the antireflective property of sample B-IV (TiO_2/SiO_2) was proved to be effective for enhancing the PCE of polycrystalline silicon solar cells.

Data Availability

The data are available within the article.

Conflicts of Interest

The authors declare that they have no conflicts of interest.

Acknowledgments

The author R. Rajasekar thanks Kongu Engineering College for providing financial support to carry out the entire research work under a Kongu Engineering College-SEED grant (proposal no. KEC/R&D/SGRS/06/2020). In addition to this, author V. K. Gobinath thanks the Department of Science & Technology (DST), Government of India, for the final completion of this research work through Teachers Associateship for Research Excellence (Ref No. TAR/2021/000173).

References

[1] I. Dincer, "Renewable energy and sustainable development: a crucial review," *Renewable and Sustainable Energy Reviews*, vol. 4, no. 2, pp. 157–175, 2000.

[2] M. S. Guney, "Solar power and application methods," *Renewable and Sustainable Energy Reviews*, vol. 57, no. 2016, pp. 776–785, 2016.

[3] N. K. Roy and A. Das, "Prospects of renewable energy sources," in *Renewable Energy and the Environment*, pp. 1–39, Springer, Berlin, Germany, 2018.

[4] S. D. Wolf, A. Descoeudres, Z. C. Holman, and C. Ballif, "High-efficiency silicon heterojunction solar cells: a review," *green*, vol. 0, no. 0, pp. 7–24, 2012.

[5] G. Velu Kaliyannan, S. V. Palanisamy, R. Rathanasamy et al., "An extended approach on power conversion efficiency enhancement through deposition of ZnS-Al2S3 blends on silicon solar cells," *Journal of Electronic Materials*, vol. 49, no. 10, pp. 5937–5946, 2020.

[6] Y. Liu, O. J. Guy, J. Patel, H. Ashraf, and N. Knight, "Refractive index graded anti-reflection coating for solar cells based on low cost reclaimed silicon," *Microelectronic Engineering*, vol. 110, pp. 418–421, 2013.

[7] J.-H. Lee, K.-H. Ko, and B.-O. Park, "Electrical and optical properties of ZnO transparent conducting films by the sol–gel method," *Journal of Crystal Growth*, vol. 247, no. 1-2, pp. 119–125, 2003.

[8] S.-Y. Lien, D.-S. Wuu, W.-C. Yeh, and J.-C. Liu, "Tri-layer antireflection coatings (SiO2/SiO2–TiO2/TiO2) for silicon solar cells using a sol–gel technique," *Solar Energy Materials and Solar Cells*, vol. 90, no. 16, pp. 2710–2719, 2006.

[9] Q. M. Wang, T. F. Zhang, S. H. Kwon, and K. H. Kim, "Fabrication of TiO2 films on glass substrates by a pulsed dc reactive magnetron sputtering," *Applied Mechanics and Materials*, vol. 71-78, pp. 5050–5053, 2011.

[10] R. Goyal, S. Lamba, and S. Annapoorni, "Growth of cobalt nanoparticles in Co–Al2O3 thin films deposited by RF sputtering," *Physica Status Solidi (A)*, vol. 213, no. 5, pp. 1309–1316, 2016.

[11] D. H. Hwang, J. H. Ahn, K. N. Hui, K. S. Hui, and Y. G. Son, "Structural and optical properties of ZnS thin films deposited by RF magnetron sputtering," *Nanoscale Research Letters*, vol. 7, no. 1, pp. 26-27, 2012.

[12] J. Li, Y. Lu, P. Lan et al., "Design, preparation, and durability of TiO2/SiO2 and ZrO2/SiO2 double-layer antireflective coatings in crystalline silicon solar modules," *Solar Energy*, vol. 89, pp. 134–142, 2013.

[13] L. Ye, Y. Zhang, X. Zhang et al., "Sol–gel preparation of SiO2/TiO2/SiO2–TiO2 broadband antireflective coating for solar cell cover glass," *Solar Energy Materials and Solar Cells*, vol. 111, pp. 160–164, 2013.

[14] A. Bahrami, S. Mohammadnejad, and S. Soleimaninezhad, "Photovoltaic cells technology: principles and recent developments," *Optical and Quantum Electronics*, vol. 45, no. 2, pp. 161–197, 2013.

[15] G. V. Kaliyannan, S. V. Palanisamy, M. Palanisamy, M. Subramanian, P. Paramasivam, and R. Rathanasamy, "Development of sol-gel derived gahnite anti-reflection coating for augmenting the power conversion efficiency of polycrystalline silicon solar cells," *Materials Science-Poland*, vol. 37, no. 3, pp. 465–472, 2019.

[16] F. C. Krebs, "Polymer solar cell modules prepared using roll-to-roll methods: knife-over-edge coating, slot-die coating and screen printing," *Solar Energy Materials and Solar Cells*, vol. 93, no. 4, pp. 465–475, 2009.

[17] S. Mukherjee and A. Mukherjee, "Scanning electron microscopy study of CVD grown MoSe2 on copper and silicon wafers," *Intl J Emerging Tech Advanced Engineering*, vol. 9, no. 12, pp. 109–112, 2019.

[18] J. R. Chi, P. Fan, G. X. Liang et al., "Room temperature deposition and properties of AZO thin films by DC magnetron sputtering under different plasma power," *Advanced Materials Research*, vol. 194-196, pp. 2440–2443, 2011.

[19] J. Puetz and M. Aegerter, "Dip coating technique," *Sol-gel Technologies for Glass Producers and Users*, pp. 37–48, Springer, Berlin, Germany, 2004.

[20] A. Tanhaei, M. Mohammadi, H. Hamishehkar, and M. R. Hamblin, "Electrospraying as a novel method of particle engineering for drug delivery vehicles," *Journal of Controlled Release*, vol. 330, pp. 851–865, 2021.

[21] C. J. Luo, S. Loh, E. Stride, and M. Edirisinghe, "Electrospraying and electrospinning of chocolate suspensions," *Food and Bioprocess Technology*, vol. 5, no. 6, pp. 2285–2300, 2012.

[22] D. Raval, J. Kabariya, T. Hazra, and V. Ramani, "A review on electrospraying technique for encapsulation of nutraceuticals," *International Journal of Communication Systems*, vol. 7, no. 5, pp. 1183–1187, 2019.

[23] R. Kessick, J. Fenn, and G. Tepper, "The use of AC potentials in electrospraying and electrospinning processes," *Polymer*, vol. 45, no. 9, pp. 2981–2984, 2004.

[24] Ö. Kesmez, E. Akarsu, H. E. Çamurlu, E. Yavuz, M. Akarsu, and E. Arpaç, "Preparation and characterization of multilayer anti-reflective coatings via sol-gel process," *Ceramics International*, vol. 44, no. 3, pp. 3183–3188, 2018.

[25] B. G. Priyadarshini and A. K. Sharma, "Design of multi-layer anti-reflection coating for terrestrial solar panel glass," *Bulletin of Materials Science*, vol. 39, no. 3, pp. 683–689, 2016.

[26] S. Sivaraj, R. Rathanasamy, G. Velu Kaliyannan, and M. Palanisamy, "Surface coatings of zinc oxide–tantalum pentoxide on multicrystalline Si solar cell as effective light harvester," *Journal of Materials Science: Materials in Electronics*, vol. 33, no. 22, pp. 17699–17710, 2022.

[27] A. K. Sharma, B. G. Priyadarshini, B. R. Mehta, and D. Kumar, "An amorphous barium titanate thin film improves light trapping in Si solar cells," *RSC Advances*, vol. 5, no. 74, pp. 59881–59886, 2015.

[28] P. P. Altermatt, "Models for numerical device simulations of crystalline silicon solar cells—a review," *Journal of Computational Electronics*, vol. 10, no. 3, pp. 314–330, 2011.

[29] A. R. Mohd Rais, N. A. Mohd Sinin, S. Sepeai, M. A. Ibrahim, S. H. Zaidi, and K. Sopian, "Analysis of spectral transmission in Si solar cell with pyramidal texturization by using PC3S simulation," *Silicon*, pp. 1–12, 2022.

[30] V. K. Gobinath, R. Rajasekar, S. Santhosh, C. Moganapriya, A. M. Sri, and S. K. Jaganathan, "An effective approach on

attaining enhanced silicon solar cell performance through sputter deposited perovskite thin films," *Silicon*, pp. 1–16, 2022.

[31] S. Dubey, J. N. Sarvaiya, and B. Seshadri, "Temperature dependent photovoltaic (PV) efficiency and its effect on PV production in the world–a review," *Energy Procedia*, vol. 33, pp. 311–321, 2013.

[32] A. S. Pugalenthi, R. Balasundaraprabhu, S. Prasanna, K. Thilagavathy, N. Muthukumarasamy, and S. Jayakumar, "Effect of substrate temperature on structural, morphology and optical properties of RF magnetron sputtered CZT thin films," *Materials Technology*, vol. 30, no. 4, pp. 200–204, 2015.